Application of the low-finesse γ-ray frequency comb for high-resolution spectroscopy

R. N. Shakhmuratov,[1,2] F. G. Vagizov,[2,3] Marlan O. Scully,[3] and Olga Kocharovskaya[3]
[1]*Kazan Physical-Technical Institute, Russian Academy of Sciences, 10/7 Sibirsky Trakt, Kazan 420029 Russia*
[2]*Kazan Federal University, 18 Kremlyovskaya Street, Kazan 420008 Russia*
[3]*Institute for Quantum Studies and Engineering and Department of Physics and Astronomy, TAMU, College Station, Texas 77843-4242, USA*
(Received 12 January 2016; published 25 October 2016)

High-finesse frequency combs (HFC) with large ratio of the frequency spacing to the width of the spectral components have demonstrated remarkable results in many applications such as precision spectroscopy and metrology. We found that low-finesse frequency combs having very small ratio of the frequency spacing to the width of the spectral components are more sensitive to the exact resonance with absorber than HFC. Our method is based on time domain measurements reviling oscillations of the radiation intensity after passing through an optically thick absorber. Fourier analysis of the oscillations allows to reconstruct the spectral content of the comb. If the central component of the incident comb is in exact resonance with the single line absorber, the contribution of the first sideband frequency to oscillations is exactly zero. We demonstrated this technique with γ-photon absorption by Mössbauer nuclei providing the spectral resolution beyond the natural broadening.

DOI: 10.1103/PhysRevA.94.043849

I. INTRODUCTION

Techniques using femtosecond-laser frequency combs allow to measure extremely narrow optical resonances with high resolution [1–4]. This is achieved by comparison of one of the spectral components of the calibrated frequency comb with the frequency of an extremely stable laser, which is tuned in resonance with the narrow absorption line under investigation. Broadband high-resolution x-ray frequency combs were proposed to be generated by the x-ray pulse shaping method, which imprints a comb on the excited transition with a high photon energy by the optical-frequency comb laser driving the transition between the metastable and excited states [5,6]. Enabling this technique in the x-ray domain is expected to result in wide-range applications, such as more precise tests of astrophysical models, quantum electrodynamics, and the variability of fundamental constants.

Special kind of γ-ray frequency combs were generated much earlier by Doppler modulation of the radiation frequency, induced by mechanical vibrations of the source or a resonant absorber [7–15] . They were observed in the frequency domain and appear only if the source and the absorber were used in a couple. Contrary to the optical and x-ray combs, discussed above, γ-ray frequency combs do not produce sharp, short pulses in time domain, except in the cases where some additional conditions are satisfied [16,17].

These special γ-ray frequency combs with high finesse $F \gg 1$, where F is the ratio of the comb-tooth spacing to the tooth width, demonstrated that in many cases determination of small energy shifts between the source and absorber can be made more accurately in the time domain by transient and high-frequency modulation techniques than by conventional methods in frequency domain [12,13,18]. In time-domain-spectroscopy technique, the γ-ray frequency comb is transmitted through a single line absorber whose resonant transition is studied. Out of resonance the phase modulation of the field, generating the frequency comb, does not produce the modulation of the field intensity at the exit of the absorber. If one of the comb components comes to resonance with the absorber, the intensity of the transmitted radiation acquires oscillations. Their pattern is very sensitive to the resonant detuning.

We have to emphasize that in γ domain even standard spectroscopic measurements with such a popular Mössbauer isotopes as ^{57}Fe and ^{67}Zn have already demonstrated extremely high-frequency resolution in measurements of gravitational redshift [19–21]. This is because the quality factor Q, which is the ratio of the resonance frequency to the linewidth, is very high for these nuclei. For example, the 14.4-keV transition in ^{57}Fe has $Q = 3 \times 10^{12}$ and the 93.3-keV resonance in ^{67}Zn demonstrates $Q = 1.8 \times 10^{15}$. Appropriate sources emitting resonant or very close to resonance γ photons with high Q are available for both nuclei. They are ^{57}Co for ^{57}Fe and ^{67}Ga for ^{67}Zn. Here we show that a low-finesse comb (LFC) with $F \ll 1$ is more sensitive to the small resonant detuning between the fundamental of the radiation field and the absorber compared with the high-finesse comb (HFC).

II. FREQUENCY COMBS IN γ DOMAIN: FREQUENCY AND TIME DOMAIN MEASUREMENTS

The basic idea of the modulation technique in γ domain is that the pistonlike vibration of an absorber leads to a periodic modulation of the resonant nuclear transition frequency with respect to the frequency of the incident photons owing to the Doppler effect. This modulation induces coherent Raman scattering of the incident radiation in the forward direction transforming a quasimonochromatic field into a frequency comb at the exit of the absorber [15]. The relative amplitudes and phases of the produced spectral components are defined by the vibration amplitude d and frequency Ω, the detuning of the central frequency of the radiation source ω_S from the resonant frequency of the absorber ω_A, the linewidths of the source Γ_S and absorber Γ_A, and the absorber optical depth T_A.

To describe the transformation of the quasimonochromatic radiation field into a frequency comb, it is convenient to consider the interaction of the field with nuclei in the reference frame rigidly bounded to the pistonlike vibrated absorber. There, nuclei "see" the quasi-monochromatic source radiation with the main frequency ω_S as polychromatic radiation with a

set of spectral lines $\omega_S \pm n\Omega$ ($n = 0,1,2,\dots$) spaced apart at distances that are multiples of the oscillation frequency. The intensity of the nth sideband is given by the square of the Bessel function $J_n^2(a)$, here $a = 2\pi d/\lambda$ is the modulation index of the field phase $\varphi(t) = a\sin(\Omega t)$, and λ is the wavelength of the radiation.

If the modulation frequency Ω is much lager than Γ_S, the power spectrum of the radiation field, seen by the absorber nuclei, demonstrates HFC ($F = \Omega/\Gamma_S \gg 1$). It is observed in many Mössbauer experiments [7–15] by transmitting the radiation field through a single line absorber with resonant frequency ω_A. The carrier frequency of the radiation frequency of the source ω_S is changed by a constant velocity Doppler shift. The intensity of the transmitted radiation, showing a frequency-comb Mössbauer spectrum, is described by equation

$$I_M(\omega_A - \omega_S) = \int_{-\infty}^{+\infty} \langle I_S(\omega)\rangle_{t_0} e^{-\alpha(\omega_A-\omega)l} d\omega, \qquad (1)$$

where $\alpha(\omega_A - \omega)$ is the frequency dependent absorption coefficient of the single line absorber, l is the absorber thickness, and $\langle I_S(\omega)\rangle_{t_0}$ is the power spectrum of the radiation field seen by the vibrated nuclei. Here, the power spectrum is averaged over the random time of photon emission t_0 (see Sec. III for details).

Frequency-domain Mössbauer spectrum is measured by counting the number of photons, detected within long time windows of the same duration for all resonant detunings, which are varied by changing the value of a constant velocity of the Mössbauer drive moving the source. Time windows are not synchronized with the mechanical vibration and their duration T_w is much longer than the oscillation period $T_{osc} = 2\pi/\Omega$.

If $F \ll 1$, the spectral components of the frequency comb, seen by the absorber nuclei, overlap resulting in the spectrum broadening of the radiation field [see Fig. 1(a)]. Therefore Mössbauer spectra for LFC show only the line broadening with increase of the modulation index a, see Fig. 1(b).

If the time windows of the photon-count collection are synchronized with the phase oscillations and the duration of the time-windows T_w is much shorter than the oscillation period T_{osc}, then one can observe time dependence of the transmitted radiation.

For HFC, the number of counts $N(t)$, proportional to the radiation intensity $I(t)$, is described by the equation [12,13,16,18]

$$N(t) = N_0 \sum_{n=0}^{\infty} D_n \cos[n\Omega(t - t_n)], \qquad (2)$$

where N_0 is the number of counts without absorber, and D_n and $n\Omega t_n$ are the amplitude and phase of the nth harmonic. Here, nonresonant absorption is disregarded. Recoil processes in nuclear absorption and emission are not taken into account assuming that recoilless fraction (Debye-Waller factor) is $f = 1$. These processes can be easily taken into account in experimental data analysis.

If the fundamental frequency ω_S of the comb coincides with the resonant frequency of the single line absorber ($\omega_S = \omega_A$), then the amplitudes of the odd harmonics are zero, $D_{2m+1} = 0$, where m is integer. They become nonzero for nonresonant excitation. For high-finesse combs, the ratio of the amplitudes of the first and second harmonics D_1/D_2 is linearly proportional to the resonant detuning $\Delta = \omega_A - \omega_S$ if the value of the modulation index a is not large and the resonant detuning does not exceed the linewidth $(\Gamma_A + \Gamma_S)/2$ [12,13]. This dependence helps to measure the value of small resonant detuning with high accuracy [18]. For HFC, the optimal value of the modulation index providing the best signal to noise ratio is $a = 1.08$ when the amplitude of the first harmonic D_1 takes maximum. This is because for HFC D_1 is proportional to the product of the amplitudes of zero and first components of the comb, i.e., to $J_0(a)J_1(a)$, which has global maximum when $a = 1.08$.

If one of the sidebands of the comb ($\omega_S \pm n\Omega$) is in resonance with the absorber ($\omega_S \pm n\Omega = \omega_A, n \neq 0$), then the time dependence of the radiation field shows large amplitude pulses of short duration [16,17]. The high sensitivity of HFC to the resonance of its central frequency with a single line absorber and the formation of short pulses if the sidebands are in resonance are explained by the interference of the spectral components of the comb, which are changed after passing through the absorber. In this paper, we show that LFC is much more sensitive to the resonance of the central component of the comb with the single line absorber. Such a sensitivity can be explained by the following arguments.

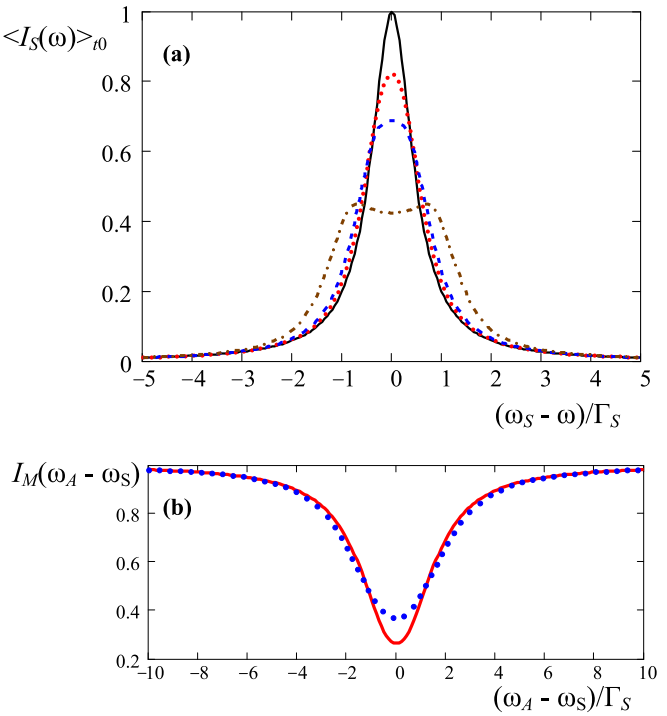

FIG. 1. (a) Power spectrum of the source radiation field, seen by the vibrated absorber (normalized to the peak intensity). (b) The absorption spectrum of the field, normalized to unity. The vibration frequency is $\Omega = \Gamma_S/5$. The modulation index a is 0 (solid line), 2 (dotted line), 3 (dashed line), and 6 (dash-dotted line) in (a). The modulation index a is 0 (solid line) and 6 (dotted line) in (b). The optical thickness of the absorber is $T_a = \alpha(0)l = 5.2$. The linewidth of the absorber Γ_A and spectral components of the source Γ_S are equal to Γ_0, which is defined by the lifetime of the excited state nucleus (141 ns).

Since the radiation intensity is $I(t) = E(t)E^*(t)$, which is the product of the complex conjugated amplitudes $E(t)$ containing the exponential phase factor $\exp[i\varphi(t)]$, the time dependent phase $\varphi(t)$ of the field amplitude does not lead to the additional time dependence of the intensity. This fact, resulting from the simple relation $e^{i\varphi(t)}e^{-i\varphi(t)} = 1$, can be explained by a particular interference of the spectral components of our specific frequency comb. For example, only the zero frequency spectral component is present in the intensity, $I(t) = I_0$, since all zero frequency spectral components, resulting from the products $e^{in\Omega t}e^{-in\Omega t}$ with $n = 0, \pm 1, \pm 2, \ldots$, are summed up with their weights as

$$\sum_{n=-\infty}^{+\infty} J_n^2(a) = 1, \tag{3}$$

while the first harmonic $I_1(t)e^{i\Omega t}$ is zero because the sum of the products of the contributing spectral components of the field amplitude gives

$$\sum_{n=-\infty}^{+\infty} J_n(a)J_{n-1}(a) = 0. \tag{4}$$

The same is true for all higher-frequency components of the intensity oscillations. This fragile balance between the spectral components of the comb is easily broken after passing through the single line absorber. We found that for LFC the absorber of thickness l satisfying the relation $\alpha(0)l = 1$ is already capable to produce noticeable time oscillations of the intensity. These oscillations are also described by Eq. (2) whose coefficients can be calculated by the method developed in Refs. [13,16] (see details in Sec. III). In contrast to HFC ($\Omega \gg \Gamma_S$), LFC ($\Omega \ll \Gamma_S$) becomes sensitive to exact resonance if the effective halfwidth of the comb $a\Omega$ is nearly equal to the width of the absorption line Γ_A. Since for LFS $a \gg 1$, much more spectral components $[J_n(a)J_{n+1}(a)$ with $n = 0, \pm 1, \ldots, \pm a]$ participate in the interference compared with HFC. Thus the spectral content of the intensity oscillations becomes more sensitive to the resonant detuning.

III. THEORETICAL MODEL

The propagation of γ radiation through a resonant Mössbauer medium vibrating with frequency Ω may be treated classically [22] . In this approach the radiation field from the source nucleus after passing through a small diaphragm is approximated as a plane wave propagating along the direction **x**. In the coordinate system rigidly bounded to the absorbing sample, the field, seen by the absorber nuclei, is described by

$$E_S(t - t_0) \propto \theta(t - t_0)e^{-(i\omega_S + \Gamma_0/2)(t-t_0)+ikx+i\varphi(t)}, \tag{5}$$

where ω_S and k are the carrier frequency and the wave number of the radiation field, $1/\Gamma_0$ is the lifetime of the excited state of the emitting source nucleus, t_0 is the instant of time when the excited state is formed, $\Theta(t - t_0)$ is the Heaviside step function, $\varphi(t) = 2\pi x_d(t)/\lambda = a\sin(\Omega t)$ is a time dependent phase of the field due to a pistonlike periodical displacement of the absorber with respect to the source, $x_d(t)$, and λ is the radiation wavelength.

It can be easily shown that radiation intensity at the exit of the vibrating absorber is the same if the source is vibrated instead of absorber. For simplicity we consider the vibration of the source with respect to the absorber and not vice versa, since both cases are equivalent. Then the radiation field from the source can be expressed as follows:

$$E_S(t - t_0) = E_C(t - t_0)e^{-i\omega_S(t-t_0)+ikx}\sum_{n=-\infty}^{+\infty} J_n(a)e^{in\Omega t}, \tag{6}$$

where $E_C(t - t_0) = E_0\theta(t - t_0)e^{-\Gamma_0(t-t_0)/2}$ is the common part of the field components, E_0 is the field amplitude, and $J_n(a)$ is the Bessel function of the nth order. The Fourier transform of this field is

$$E_S(\omega) = E_0\sum_{n=-\infty}^{+\infty}\frac{J_n(a)e^{in\Omega t_0}}{\Gamma_0/2 + i(\omega_S - n\Omega - \omega)}, \tag{7}$$

where for shortening of notations the exponential factor with ikx is omitted. From this expression, it is clear that the vibrating absorber "sees" the incident radiation as an equidistant frequency comb with spectral components $\omega_S - n\Omega$ whose amplitudes are proportional to the Bessel function $J_n(a)$. Below, for briefness we use the shortened notation $J_n(a) = J_n$.

According to Eq. (5) the intensity of the field

$$I(t - t_0) = |E_S(t - t_0)|^2 = I_0\theta(t - t_0)e^{-\Gamma_0(t-t_0)}, \tag{8}$$

where $I_0 = E_0^2$, does not oscillate in time. The same result must be obtained from Eq. (6), which gives

$$|E_S(t - t_0)|^2 = |E_C(t - t_0)|^2\sum_{n=-\infty}^{+\infty}\sum_{m=-\infty}^{+\infty} J_nJ_me^{i(n-m)\Omega t}, \tag{9}$$

where $|E_C(t - t_0)|^2 = I_0(t - t_0)$ according to the definition. Therefore the identity

$$\sum_{n=-\infty}^{+\infty}\sum_{m=-\infty}^{+\infty} J_nJ_me^{i(n-m)\Omega t} = 1 \tag{10}$$

is to be satisfied. It is consistent with the well known relations between the Bessel functions (see, for example, Ref. [23]). They are

$$\sum_{n=-\infty}^{+\infty} J_n^2 = J_0^2 + 2\sum_{n=1}^{+\infty} J_n^2 = 1 \tag{11}$$

for zero harmonic ($n = m$), which is the only harmonic giving nonzero contribution into the radiation intensity in Eq. (9) due to Eq. (10), and

$$\sum_{n=-\infty}^{+\infty} J_nJ_{n+2} = -J_1^2 + 2\sum_{n=0}^{+\infty} J_nJ_{n+2} = 0, \tag{12}$$

for the second harmonic (-2Ω) with $m = n + 2$ in Eq. (9), and

$$\sum_{n=-\infty}^{+\infty} J_nJ_{n+4} = J_2^2 - 2J_1J_3 + 2\sum_{n=0}^{+\infty} J_nJ_{n+4} = 0, \tag{13}$$

for the fourth harmonic (-4Ω) with $m = n + 4$. It can be easily shown that all even harmonics do not contribute since their amplitudes are zero. As regards the odd harmonics, they have

zero amplitudes because of the cancelation of the symmetric pairs in their content as, for example, for the first harmonic $(-\Omega)$ with $m = n + 1$,

$$\sum_{n=-\infty}^{+\infty} J_n J_{n+1} = (J_0 J_1 + J_{-1} J_0) + (J_1 J_2 + J_{-2} J_{-1}) + \ldots = 0, \quad (14)$$

and the third harmonic (-3Ω) with $m = n + 3$,

$$\sum_{n=-\infty}^{+\infty} J_n J_{n+3} = (J_0 J_3 + J_{-3} J_0) + (J_1 J_4 + J_{-4} J_{-1}) + \ldots = 0. \quad (15)$$

Here the property of the Bessel function, $J_{-n} = (-1)^n J_n$ (where n is positive), is taken into account. If such a field with balanced amplitudes and phases of its harmonics, Eq. (6), passes through a thick resonant absorber, one may expect that this balance will be broken and the intensity of the field at the exit of the absorber will be oscillating.

A. The transformation of the radiation field after passing through a resonant absorber

The Fourier transform of the radiation field is changed at the exit of the resonant absorber as (see Refs. [13,16])

$$E_{\text{out}}(\omega) = E_0 \sum_{n=-\infty}^{+\infty} \frac{J_n \exp\left[in\Omega t_0 - \frac{b}{\Gamma_A/2 + i(\omega_A - \omega)}\right]}{\Gamma_0/2 + i(\omega_S - n\Omega - \omega)}, \quad (16)$$

where ω_A and Γ_A are the frequency and linewidth of the absorber, $b = T_A\Gamma_0/4$ is the parameter depending on the effective thickness of the absorber $T_A = f n_A \sigma$, f is the Debye-Waller factor, n_A is the number of ^{57}Fe nuclei per unit area of the absorber, and σ is the resonance absorption cross section. The source linewidth Γ_S can be different from Γ_0 due to the contribution of the environment of the emitting nucleus in the source. In this case Γ_0 can be simply substituted by Γ_S in Eq. (16).

Time dependence of the amplitude of the output radiation field is found by inverse Fourier transformation

$$E_{\text{out}}(t - t_0) = \frac{1}{2\pi} \int_{-\infty}^{+\infty} E_{\text{out}}(\omega) e^{-i\omega(t-t_0)} d\omega. \quad (17)$$

Then, the intensity of the field is

$$I_{\text{out}}(t - t_0) = \frac{1}{(2\pi)^2} \int_{-\infty}^{+\infty} d\omega_1 \int_{-\infty}^{+\infty} d\omega_2 E_{\text{out}}(\omega_1) E^*_{\text{out}}(\omega_2) \times e^{i(\omega_2 - \omega_1)(t-t_0)}. \quad (18)$$

In time domain experiments, the phase of the vibrations is fixed but emission time of γ-photons is random. Therefore the observed radiation intensity is averaged over t_0:

$$\langle I_{\text{out}}(t - t_0)\rangle_{t_0} = \lim_{T\to\infty} \int_{-T}^{t} I_{\text{out}}(t - t_0) dt_0. \quad (19)$$

Calculation of this integral gives for the number of γ-photon counts at the exit of the absorber, $N_{\text{out}}(t) \propto \langle I_{\text{out}}(t - t_0)\rangle_{t_0}$, the following expression (see [16]):

$$N_{\text{out}}(t)/N_0 = \sum_{n,m=-\infty}^{+\infty} J_n J_m e^{i(n-m)\Omega t} B_{nm}(\Delta), \quad (20)$$

where N_0 is the number of counts far from resonance and

$$B_{nm}(\Delta) = \frac{\Gamma_S}{2\pi} \int_{-\infty}^{+\infty} \frac{e^{-\frac{b}{\Gamma_A/2 + i(\Delta + n\Omega - \omega)} - \frac{b}{\Gamma_A/2 - i(\Delta + m\Omega - \omega)}}}{(\Gamma_S/2)^2 + \omega^2} d\omega, \quad (21)$$

where $\Delta = \omega_A - \omega_S$ is the resonance detuning of the source and absorber. In derivation of Eq. (21) the substitution $\omega' = \omega - \omega_S + n\Omega$ is used in Eqs. (16) and (18). Then the prime is omitted.

B. Intensity oscillations

To analyze the oscillations of the radiation intensity after passing through the vibrated absorber it is convenient to group the terms in Eq. (20) as follows:

$$N_{\text{out}}(t)/N_0 = \mathtt{I}_0(\Delta) + 2\,\text{Re} \sum_{n=1}^{+\infty} \mathtt{I}_n(\Delta) e^{-in\Omega t}, \quad (22)$$

where $\mathtt{I}_n(\Delta)$ is the nth-harmonic amplitude of the radiation intensity oscillations at the exit of the absorber. The amplitudes of the harmonics are defined by the products of the radiation amplitudes of the frequency comb (16), transformed by the absorber. For example, the amplitude of zero harmonic is

$$\mathtt{I}_0(\Delta) = J_0^2 B_{00}(\Delta) + \sum_{n=1}^{+\infty} J_n^2 [B_{nn}(\Delta) + B_{(-n)(-n)}(\Delta)], \quad (23)$$

where the coefficients $B_{00}(\Delta)$, $B_{nn}(\Delta)$, and $B_{(-n)(-n)}(\Delta)$ are transmitted intensities of 0, n, and $-n$ components of the incident comb (6). They are

$$B_{00}(\Delta) = \frac{\Gamma_S}{2\pi} \int_{-\infty}^{+\infty} \frac{e^{-\frac{b\Gamma_A}{(\Gamma_A/2)^2 + (\Delta - \omega)^2}}}{(\Gamma_S/2)^2 + \omega^2} d\omega, \quad (24)$$

$$B_{(\pm n)(\pm n)}(\Delta) = \frac{\Gamma_S}{2\pi} \int_{-\infty}^{+\infty} \frac{e^{-\frac{b\Gamma_A}{(\Gamma_A/2)^2 + (\Delta \pm n\Omega - \omega)^2}}}{(\Gamma_S/2)^2 + \omega^2} d\omega. \quad (25)$$

Thus $\mathtt{I}_0(\Delta)$ is just the sum of the transmitted intensities of all spectral components of the frequency comb (6).

The first harmonic

$$\mathtt{I}_1(\Delta) = \sum_{n=0}^{+\infty} J_n J_{n+1} [B_{n(n+1)}(\Delta) - B_{(-n-1)(-n)}(\Delta)], \quad (26)$$

contains the difference of two terms originating from the interference of two neighboring components of the frequency comb $\pm n$ and $\pm(n + 1)$. They are red (for sign $+$) and blue (for sign $-$) detuned from resonance. This difference is

$$B_{n(n+1)}(\Delta) - B_{(-n-1)(-n)}(\Delta) = \frac{\Gamma_S}{2\pi} \int_{-\infty}^{+\infty} \frac{e^{-\frac{b}{\Gamma_A/2 + i(\Delta + n\Omega - \omega)} - \frac{b}{\Gamma_A/2 - i[\Delta + (n+1)\Omega - \omega]}} - e^{-\frac{b}{\Gamma_A/2 + i[\Delta - (n+1)\Omega - \omega]} - \frac{b}{\Gamma_A/2 - i(\Delta - n\Omega - \omega)}}}{(\Gamma_S/2)^2 + \omega^2} d\omega. \quad (27)$$

It is easy to show (by substitution $\omega = -\omega'$ in the second exponent) that the difference of the interference terms is zero if $\Delta = 0$.

The second and third harmonics are described by equations

$$\mathtt{I}_2(\Delta) = -J_1^2 B_{-11}(\Delta) + \sum_{n=0}^{+\infty} J_n J_{n+2}[B_{n(n+2)}(\Delta) + B_{(-n-2)(-n)}(\Delta)], \quad (28)$$

$$\mathtt{I}_3(\Delta) = -J_1 J_2[B_{-12}(\Delta) - B_{-21}(\Delta)] + \sum_{n=0}^{+\infty} J_n J_{n+3}[B_{n(n+3)}(\Delta) - B_{(-n-3)(-n)}(\Delta)], \quad (29)$$

which contain the interference terms of the frequency-comb amplitudes with $m - n = 2$ for $\mathtt{I}_2(\Delta)$ and $m - n = 3$ for $\mathtt{I}_3(\Delta)$ [see Eq. (21)]. The third harmonic is zero if $\Delta = 0$ because it contains the difference of the interference terms, while the second harmonic is not zero since it is the sum of the interference terms.

The coefficients D_n in Eq. (2), describing the number of count oscillations in time, are related to the harmonics $\mathtt{I}_n(\Delta)$ as $D_0 = \mathtt{I}_0(\Delta)$, $D_{2n} = 2|\mathtt{I}_{2n}(\Delta)|$, and $D_{2n+1} = 2S(\Delta)|\mathtt{I}_{2n+1}(\Delta)|$, where $S(\Delta) = \Delta/|\Delta|$. The phases of the harmonics are defined as $\Omega t_n = \arctan[\mathrm{Im}\,\mathtt{I}_n(\Delta)/\mathrm{Re}\,\mathtt{I}_n(\Delta)]$.

C. High-finesse frequency comb

If the modulation frequency is much larger than the absorption linewidth ($\Omega \gg \Gamma_A$) and the central frequency of the comb ω_S is close to the resonant frequency of the absorber ω_A ($|\Delta| < \Gamma_A$), then only the central frequency of the comb is changed after passing through a thick absorber. Therefore one may expect that in Eq. (20) only the components B_{00}, B_{0n} and B_{n0} become different from 1, while others are almost unity since for them the exponents in the integral (21) are unity if the condition $n\Omega \gg b$ is satisfied. In this case, we can use approximate equations

$$\mathtt{I}_0(\Delta) \approx 1 - J_0^2[1 - B_{00}(\Delta)], \quad (30)$$

$$\mathtt{I}_1(\Delta) \approx J_0 J_1[B_{01}(\Delta) - B_{-10}(\Delta)], \quad (31)$$

$$\mathtt{I}_2(\Delta) \approx J_0 J_2[B_{02}(\Delta) + B_{-20}(\Delta) - 2], \quad (32)$$

which are derived taking into account the relations (11), (12), and (13). The product $J_0 J_1 = J_0(a)J_1(a)$ in Eq. (31) has global maximum when the modulation index is $a = 1.08$. Therefore, for nonresonant excitation ($\Delta \neq 0$ and $|\Delta| < \Gamma_A$), the first harmonic of the intensity oscillations has maximum amplitude for this value of the modulation index. Since it is not large, we may approximate the intensity oscillations taking into account only three harmonics $n = 0,1,2$ in Eq. (22).

However, to achieve high accuracy, we have to take into account also the contribution of two spectral components of the comb, neighboring the resonant component (see Ref. [17]). This is because far wings of the Lorentzian line give small, but noticable contribution. In our case, when the central component of the comb is in resonance, these nearest components are $+\Omega$ and $-\Omega$. Then, for example, $\mathtt{I}_0(\Delta)$ is modified due to this small nonresonant contribution as

$$\mathtt{I}_0(\Delta) = 1 - J_0^2[1 - B_{00}(\Delta)] - J_1^2[2 - B_{11}(\Delta) - B_{-1-1}(\Delta)]. \quad (33)$$

The value of the correction due to the additional terms is about 2% if $\Omega = 10\Gamma_0$, $\Delta = 0.2\Gamma_0$, and $T_A = 5$.

In conclusion of this subsection, we show in Fig. 2 two examples of the intensity oscillations (not approximated) for $\Gamma_A = \Gamma_S = \Gamma_0 = 1.13$ MHz, $T_A = 5.2$, $\Omega = 10$ MHz, $a = 1.08$, and $\Delta = \pm 200$ kHz. The dependence of D_1/D_2 on Δ (not approximated) is shown in Fig. 5.

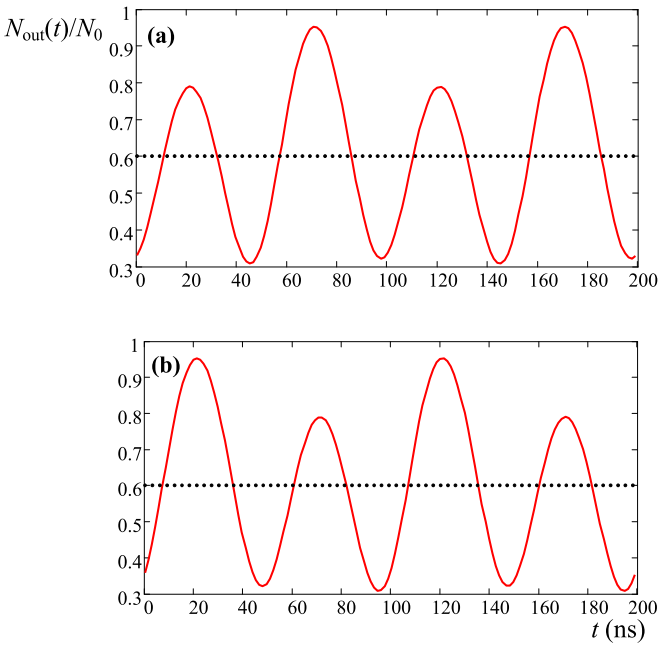

FIG. 2. Oscillations of the intensity of high-finesse frequency comb, transmitted through the absorber. Phase modulation frequency is $\Omega = 10$ MHz. Intensity oscillations are shown by solid lines for the detuning from resonance (a) $\Delta = -200$ and (b) 200 kHz. Dotted line shows the level of $\mathtt{I}_0(\Delta)$. The value of the parameters are given in the text.

D. Low-finesse comb

For the low-finesse comb, the modulation frequency is much smaller than the absorption linewidth ($\Omega \ll \Gamma_A$). If the central frequency of the comb ω_S is close to the resonant frequency of the absorber ω_A ($|\Delta| < \Gamma_A$), then many spectral components of the comb are changed after passing through a thick absorber. Therefore, to describe the oscillation of the output radiation intensity, we have to take many terms in the equations (23), (26), (28), and (29) for $\mathtt{I}_n(\Delta)$, $n = 0,1,2,3$.

Intuitively, one may expect that LFC sensitivity is maximal if all noticeable components of the comb are modified after passing through the absorber. This takes place if the product $a\Omega$, which specifies the total spectral width of the comb or the frequency range, covered by the comb components with noticeable amplitudes, is close to the width of the absorption line. Mathematically, this expectation can be verified by plotting the amplitude $D_1 = 2S(\Delta)|\mathtt{I}_1(\Delta)|$ versus modulation index a for a fixed values of the modulation frequency Ω and

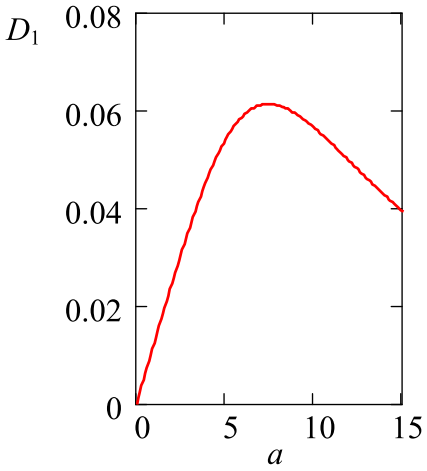

FIG. 3. The dependence of the first-harmonic amplitude D_1 of the intensity oscillations on the modulation index a. The modulation frequency and resonant detuning are $\Omega = \Delta = 200$ kHz.

resonant detuning Δ. Figure 3 shows the dependence of D_1 on the modulation index a for $\Omega = \Delta = 200$ kHz and $T_A = 5.2$. The amplitude D_1 takes maximum value when $a = 7$. For this value, the product $a\Omega$ is close to the linewidth of the absorber Γ_A.

IV. EXPERIMENT

We demonstrated LFC sensitivity in the experiments with the radiation source, which is a radioactive ^{57}Co incorporated into rhodium matrix. The source emits 14.4-keV photons with the spectral width $\Gamma_S = 1.13$ MHz, which is mainly defined by the lifetime of 14.4-keV excited state of ^{57}Fe, the intermediate state in the cascade decay of ^{57}Co to the ground state ^{57}Fe. The absorber is a 25-μm-thick stainless-steel foil with a natural abundance ($\sim$2%) of ^{57}Fe. Optical depth of the absorber is $T_A = \alpha(0)l = 5.18$. The stainless-steel foil is glued on the polyvinylidene fluoride piezotransducer that transforms the sinusoidal signal from radio-frequency generator into the uniform vibration of the foil. The frequency and amplitude of the sinusoidal voltage were adjusted to have $\Omega = 200$ kHz and $a = 5.7$, so that relation $a\Omega \approx \Gamma_A$ was satisfied. The source is attached to the holder of the Mössbauer transducer causing Doppler shift of the radiation field to tune the source in resonance or out of resonance with the single line absorber. The time measurements were performed by means of the time–amplitude converter (TAC) working in the start-stop mode. The start pulses for the converter were synchronized with radio-frequency generator and the stop pulses were formed from the signal of 14.4 keV γ counter at the instant of photon detection time. A detailed description of the experimental setup is given in Refs. [16,17].

The experimental results demonstrating the oscillations of the radiation intensity in time for different values of the resonant detunings Δ are shown in Fig. 4. Time dependence of the number of counts is fitted to Eq. (2) (see details in Sec. III). At exact resonance ($\Delta = 0$), only even harmonics are not zero. Time delay of the second harmonic with respect to the vibration phase is $t_2 = 61$ ns. This delay is caused

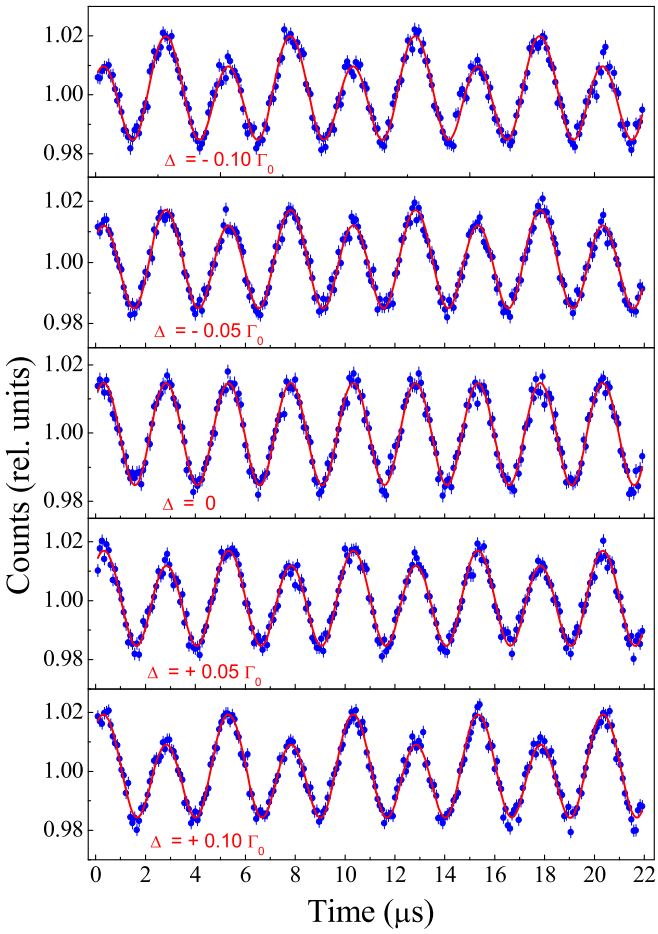

FIG. 4. Time dependence of the photon counts $N(t)$ for different values of the resonant detuning. The number of counts (in relative units) are normalized to the mean value at exact resonance. The value of the detuning in units of Γ_0 is indicated in each panel. The dots are experimental points and solid line is a theoretical fitting.

by the contribution of dispersion, which produces a phase shift $2\Omega t_2$. The Fourier analysis of the oscillations allows to reconstruct the dependence of the ratio D_1/D_2 on Δ, which is shown in Fig. 5, left panel. This dependence is compared with that for HFC, generated by the vibration with high frequency $\Omega = 10$ MHz and optimal value of the modulation index $a = 1.08$. We see that LFC is at least two times more sensitive to resonance than HFC since the slope of the dependence of D_1/D_2 on Δ is two times steeper.

Figure 5, right panel, shows the Fourier content of the oscillations of the radiation intensity for LFC when $\Delta = 0.3\Gamma_0$. The spectrum of these oscillations contains noticable contributions of the first, second, and third harmonics. The width of these spectral components is defined by the length of the time window where the oscillations are measured. In our experiments, the spectral width of each Fourier component is close to 10 kHz. Thus we may conclude that within a moderate time of experiment the proposed method is able to measure the resonant detuning for ^{57}Fe with the accuracy of 10 kHz, which is 100 times smaller than the absorption linewidth. This is essentially better accuracy than in the method, used in the gravitational red-shift measurements [19,20], which employs

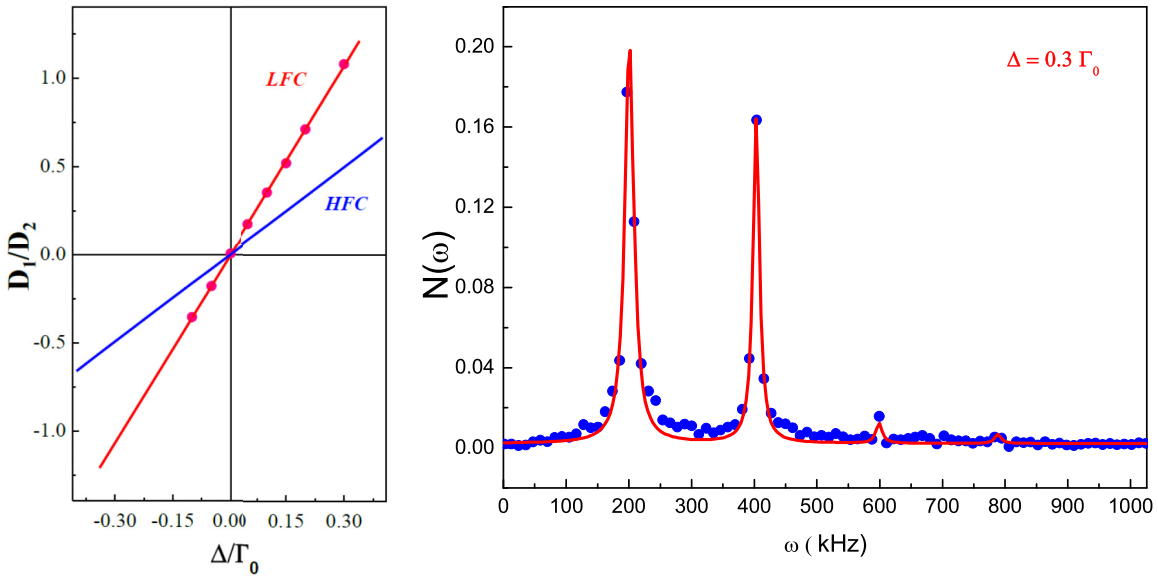

FIG. 5. (Left) Comparison of the dependence of D_1/D_2 on Δ for LFC and HFC. Experimental data for LFC are shown by dots. (Right) Fourier content of the intensity oscillations for $\Delta = 0.3\Gamma_0$. Other parameters are defined in the text. Dots correspond to the data, obtained from the Fourier analysis of the experimentally observed intensity oscillations. Solid line is the analytical approximation by the set of Lorentzians.

four known values of the calibrated, controllable resonant detunings: two very large, comparable with the halfwidth of the absorption line, and two very small, comparable but appreciably exceeding the measured detuning. In time domain measurements, by extending considerably the length of the time window where the oscillations are collected, one can reach even higher accuracy of 10^{-18} with a quite simple technique. In these experiments the regular signal grows as N, while the noise level rises as $\sqrt{N}$, where N is the number of detected photons. Therefore, to detect a very small detuning, which gives a regular signal with the amplitude of 1%, we have to collect 10^4 counts in each time bin of our data acquisition system. This condition sets a limit on the accuracy of our method since experiments cannot last infinite time. The other technical limitations are well described in Refs. [19–21] and they are related to the stability of temperature and fine calibration of the mechanical parts of the experimental setup.

V. CONCLUSION

We demonstrate a method to measure precisely the resonant frequency of the absorber with LFC, with an accuracy equal to a tiny fraction of the homogeneous absorption width. This method is also applicable in the optical domain. The modulation of the resonant frequency of atoms or impurity ions by Stark or Zeeman effects or the modulation of the frequency of the laser beam by an acousto-optical modulator are equivalent to the creation of a frequency comb in a particular reference frame. The interference of the scattered radiation field with the incident field is capable to produce the output intensity oscillations. By a proper choice of the modulation frequency and the modulation index, one can make these oscillations to be very sensitive to exact resonance or to measure the frequency difference between the incident radiation and the resonance frequency of atoms with the accuracy not limited by the value of the homogeneous linewidth.

ACKNOWLEDGMENTS

This work was partially funded by the Russian Foundation for Basic Research (Grant No. 15-02-09039-a), the Program of Competitive Growth of Kazan Federal University funded by the Russian Government, the RAS Program "Fundamental optical spectroscopy and its applications," the National Science Foundation (Grant No. PHY-1307346), and the Robert A. Welch Foundation (Award A-1261).

[1] Th. Udem, R. Holzwarth, and T. W. Hänsch, Nature (London) **416**, 233 (2002).
[2] S. T. Cundiff and J. Ye, Rev. Mod. Phys. **75**, 325 (2003).
[3] T. W. Hänsch, *Passion for Precision*, Nobel lecture, December 8, 2005.
[4] J. L. Hall, *Defining and Measuring Optical Frequencies: the Optical Clock Opportunity - and More*, Nobel lecture, December 8, 2005.
[5] S. M. Cavaletto, Z. Harman, C. Ott, C. Buth, T. Pfeifer, and C. H. Keitel, Nat. Photon. **8**, 520 (2014).
[6] Z. Liu, C. Ott, S. M. Cavaletto, Z. Harman, C. H. Keitel, and T. Pfeifer, New J. Phys. **16**, 093005 (2014).
[7] T. E. Cranshaw and P. Reivari, Proc. Phys. Soc. **90**, 1059 (1967).
[8] S. L. Ruby and D. I. Bolef, Phys. Rev. Lett. **5**, 5 (1960).
[9] G. Kornfeld, Phys. Rev. **177**, 494 (1969).

[10] J. Mishroy and D. I. Bolef, *Mössbauer Effect Methodology*, edited by I. J. Gruverman (Plenum Press, Inc., New York, 1968), Vol. 4, pp. 13–35.
[11] C. L. Chein and J. C. Walker, Phys. Rev. B **13**, 1876 (1976).
[12] G. J. Perlow, Phys. Rev. Lett. **40**, 896 (1978).
[13] J. E. Monahan and G. J. Perlow, Phys. Rev. A **20**, 1499 (1979).
[14] S. L. Popov, G. V. Smirnov, and Y. V. Shvyd'ko, Pis'ma Zh. Eksp. Teor. Fiz. **49**, 651 (1989) [JETP Lett. **49**, 747 (1989)].
[15] Yu. V. Shvyd'ko and G. V. Smirnov, J. Phys.: Condens. Matter **4**, 2663 (1992).
[16] F. Vagizov, V. Antonov, Y. V. Radeonychev, R. N. Shakhmuratov, and O. Kocharovskaya, Nature (London) **508**, 80 (2014).
[17] R. N. Shakhmuratov, F. G. Vagizov, V. A. Antonov, Y. V. Radeonychev, M. O. Scully, and O. Kocharovskaya, Phys. Rev. A **92**, 023836 (2015).
[18] P. Helistö, E. Ikonen, T. Katila, W. Potzel, and K. Riski, Phys. Rev. B **30**, 2345 (1984).
[19] T. E. Cranshaw and J. P. Schiffer, Proc. Phys. Soc. **84**, 245 (1964).
[20] R. V. Pound and J. L. Snider, Phys. Rev. **140**, B788 (1965).
[21] W. Potzel, C. Schäfer, M. Steiner, H. Karzel, W. Schiessl, M. Peter, G. M. Kalvius, T. Katila, E. Ikonen, P. Helistö, and J. Hietaniemi, Hyperfine Interactions **72**, 195 (1992).
[22] E. Ikonen, P. Helistö, T. Katila, and K. Riski, Phys. Rev. A **32**, 2298 (1985).
[23] *Handbook of Mathematical Functions*, edited by M. Abramowitz and I. A. Stegun (Dover, New York, 1965).